

# Journal of Biomedical Optics

BiomedicalOptics.SPIEDigitalLibrary.org

## **Study of smartphone suitability for mapping of skin chromophores**

Ilona Kuzmina  
Matiss Lacis  
Janis Spigulis  
Anna Berzina  
Lauma Valeine

# Study of smartphone suitability for mapping of skin chromophores

Ilona Kuzmina,<sup>a,\*</sup> Matiss Lacis,<sup>a</sup> Janis Spigulis,<sup>a</sup> Anna Berzina,<sup>b</sup> and Lauma Valeine<sup>c</sup>

<sup>a</sup>University of Latvia, Institute of Atomic Physics and Spectroscopy, Biophotonics Laboratory, Raina Boulevard 19, Riga LV-1586, Latvia

<sup>b</sup>The Clinic of Laser Plastics, Baznīcas Street 31, Riga LV-1010, Latvia

<sup>c</sup>Beauty Clinic "4th Dimension", Pulkveža Brieža Street 15, Riga LV-1010, Latvia

**Abstract.** RGB (red-green-blue) technique for mapping skin chromophores by smartphones is proposed and studied. Three smartphones of different manufacturers were tested on skin phantoms and *in vivo* on benign skin lesions using a specially designed light source for illumination. Hemoglobin and melanin indices obtained by these smartphones showed differences in both tests. *In vitro* tests showed an increment of hemoglobin and melanin indices with the concentration of chromophores in phantoms. *In vivo* tests indicated higher hemoglobin index in hemangiomas than in nevi and healthy skin, and nevi showed higher melanin index compared to the healthy skin. Smartphones that allow switching off the automatic camera settings provided useful data, while those with "embedded" automatic settings appear to be useless for distant skin chromophore mapping. © 2015 Society of Photo-Optical Instrumentation Engineers (SPIE) [DOI: 10.1117/1.JBO.20.9.090503]

Keywords: optics; photonics; skin chromophores; smartphone; skin diagnostics.

Paper 150496LR received Jul. 29, 2015; accepted for publication Aug. 28, 2015; published online Sep. 25, 2015.

## 1 Introduction

Due to growing numbers of new cases and mortality from skin cancer,<sup>1,2</sup> fast primary skin diagnostics is important. In addition to widely used dermatoscopes, some other commercial optical devices are also available for skin diagnostics in clinics.<sup>3–7</sup> These devices use visible and near-infrared light sources used to analyze skin-reflected spectral images. Due to the rapid development of smartphones and tablet PCs, many software applications are available for health assessment from images or videos taken by a smartphone camera in ambient light or a light-emitting diode (LED) light of the same phone.<sup>8–10</sup> These applications provide information about health conditions such as heart and breathe rate,<sup>8,9</sup> or malignancy of skin lesions.<sup>10</sup> Cell phone cameras have also been tested for reflectance photoplethysmographic video imaging.<sup>11</sup> We present a technique for mapping the main skin chromophores by means of an RGB light source specially designed for smartphones and tablet PCs, and

appropriate software. The suitability of three smartphone models for this application has been studied.

## 2 Materials and Methods

### 2.1 Illumination Source

An LED ring specially designed for smartphones was used in this study as a light source. The ring included four types of LEDs (four diodes of each type): white—to find and adjust the location of the skin malformation, and RGB—with emission in blue (maximum at 460 nm), green (maximum at 535 nm), and red (maximum at 663 nm) spectral regions for calculation of skin chromophore distributions. The setup scheme is presented in Fig. 1(a) and the color LED emission spectra are shown in Fig. 1(b). LEDs operated in continuous mode and were switched on and off manually or by special software. The LED ring surrounded the rear camera of the smartphone; illumination and detection were performed normal to the surface of samples. Two orthogonally oriented polarizers were used in front of the LEDs and smartphone camera, respectively, to reduce the detection of specular reflection. Five AA 2800 mAh battery blocks were used as a power supply.

### 2.2 In Vitro and In Vivo Tests

The proposed light source was tested with photo cameras of three different smartphones: LG Nexus 5 (Nexus), Samsung Galaxy Core (Galaxy), and Sony Xperia™ Go (Xperia™). Since the spectral characteristics of these cameras were not available, the first test was made on ColorChecker® (X-rite) to compare the RGB values of each smartphone camera with the tabulated values of the checker. For this purpose, three ColorChecker® squares were used: red (R-175, G-54, B-60), green (R-70, G-148, B-73), and blue (R-56, G-61, B-150).

*In vitro* tests were performed on liquid skin phantoms. The base of the phantoms was tap water with dissolved hemoglobin (hemoglobin human—lyophilized powder, Sigma-Aldrich®) and nigrosin (water soluble, Sigma-Aldrich®) to imitate absorption of skin hemoglobin and melanin, respectively. Nigrosin and melanin have similar absorption spectra at the wavelength range behind 570 nm; therefore, nigrosin was considered as an acceptable substance to mimic melanin in the phantoms.<sup>12,13</sup> Initially, intralipid (20%, emulsion) was added to the phantoms at low concentrations to mimic skin scattering; however, it did not substantially change the spectral distribution of the reflected light, so the test measurements were taken without additional scatterers in the phantoms. The liquid phantoms were filled in Petri dishes with a diameter of 5.5 cm; the height of each phantom was approximately 0.7 cm. Several hemoglobin (1% to 10%, 0.2 to 1.82 mg/ml) and nigrosin (0.1% to 1.5%, 0.01 to 0.15 mg/ml) concentrations in phantoms were chosen for the tests.

*In vivo* images of five nevi, five hemangiomas, and healthy skin were taken using the three smartphones. All pictures were taken using the following settings of the phones: ISO—100, white balance—daylight, focus—manual. In the case of the Nexus smartphone, the ISO and white balance remained automatic because it was impossible to switch it off or change it. This study was approved by the Ethics Committee of the Institute of Experimental and Clinical Medicine, University

\*Address all correspondence to: Ilona Kuzmina, E-mail: [ilona.kuzmina@lu.lv](mailto:ilona.kuzmina@lu.lv)

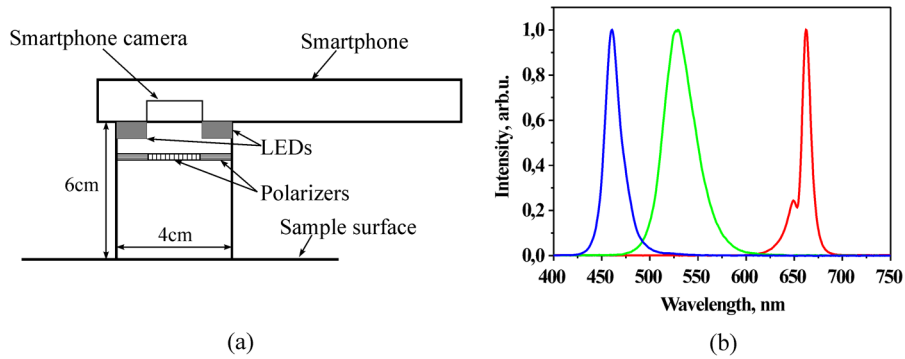


**Fig. 1** (a) Scheme of the measurement setup and (b) normalized spectra of the RGB light emitting diodes; peaks of the curves are separated.

of Latvia. All involved volunteers were informed about the study and signed the required consent.

**2.3 Processing Algorithms**

The values of RGB components were defined from the image data by a special program developed in MATLAB®. The region of interest was manually chosen from the image of a particular component (R, G, or B), and the mean value of this component was calculated. Hemoglobin and melanin indices were calculated from the mean values of the RGB components using equations adapted from the literature:<sup>14</sup>  $I_{Hb} = A \cdot (R/G)$ ,  $I_{Mel} = A \cdot (B/R)$ , where  $R$  is the mean value of the red component,  $G$  is the mean value of the green component,  $B$  is the mean value of the blue component, and  $A$  is the calibration constant.

**3 Results**

Table 1 shows the correction coefficients for three smartphones obtained from the ColorChecker® RGB measurements by

**Table 1** Correction coefficients for photo cameras of smartphones.

Color component	Correction coefficients		
	Galaxy	Nexus	Xperia™
R	$0.72 \pm 0.05$	$0.69 \pm 0.05$	$0.69 \pm 0.05$
G	$0.77 \pm 0.05$	$0.73 \pm 0.05$	$0.69 \pm 0.05$
B	$0.61 \pm 0.05$	$0.59 \pm 0.05$	$0.59 \pm 0.05$

illuminating the color checker area with LEDs of the same color. For example, the correction coefficient for the  $R$  component was obtained by illuminating the  $R$ -area of the ColorChecker® with red LEDs, and the acquired  $R$  value was divided by the tabulated  $R$  value of this area.

Figure 2 illustrates the images taken from a skin nevus in white, red, green, and blue light, as well as the map of hemoglobin index. The dependences of hemoglobin index ( $I_{Hb}$ ) on hemoglobin concentration (a) and melanin index ( $I_{Mel}$ ) on nigrosin concentration (b) in phantoms are shown in Fig. 3. The values of hemoglobin index increased with hemoglobin concentration in phantoms for all three smartphones. At hemoglobin concentrations higher than 1 mg/ml, the index increased more prominently for Galaxy than for the other two phones, while the curve of the Xperia™ phone had a shallower slope compared to others. The values of melanin index increased with nigrosin concentration in phantoms for the Galaxy and Xperia™ phones, while for the Nexus phone changes of this index were negligible.

The hemoglobin and melanin indices of healthy skin, nevi, and hemangiomas obtained by three smartphones are compared in Fig. 4. Mean values of  $I_{Hb}$  show differences among the three tested phones. The lowest values are observed for the Xperia™ phone, while Nexus and Galaxy indicate more similarities. Differences of indices among smartphones could be explained by the different spectral sensitivities of the smartphones' cameras.

As for the melanin index in nevi, Galaxy and Xperia™ phones showed higher values than for healthy skin, whereas the Nexus phone provided very similar values for both healthy skin and nevi; these values were at the same level as the  $I_{Mel}$  of skin obtained by the other two smartphones.

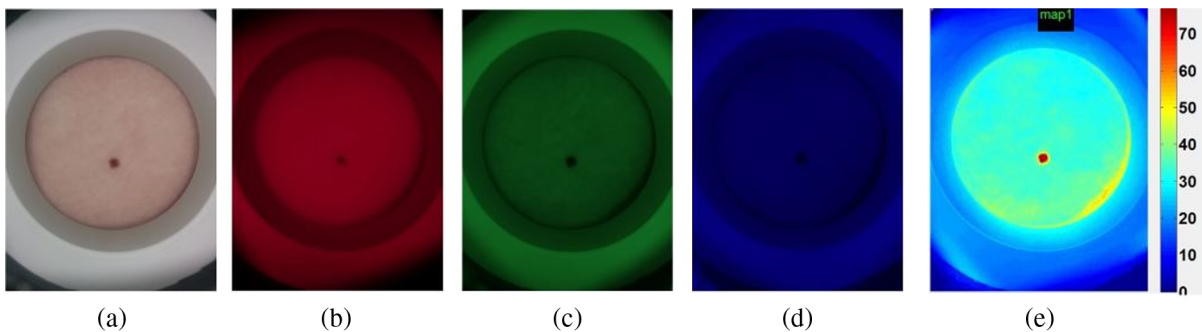


**Fig. 2** Images of a skin nevus in (a) white, (b) red, (c) green, (d) blue light, and (e) a map of hemoglobin index.

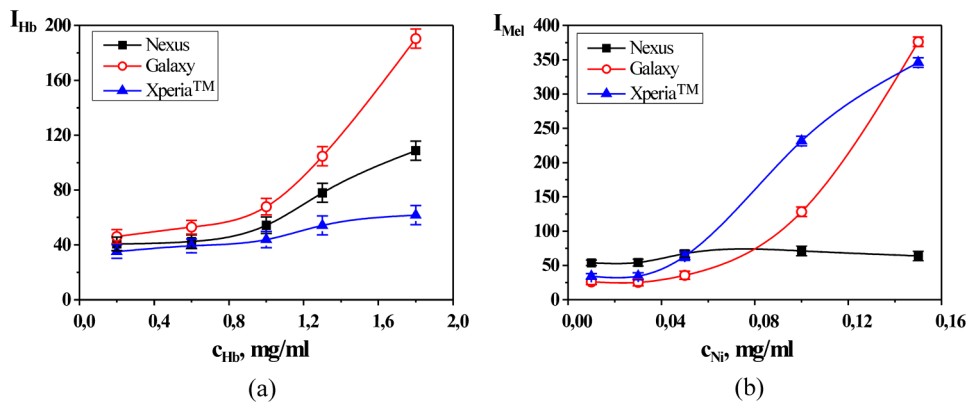


Fig. 3 Concentration dependences on (a) hemoglobin and (b) melanin indices measured in skin phantoms.

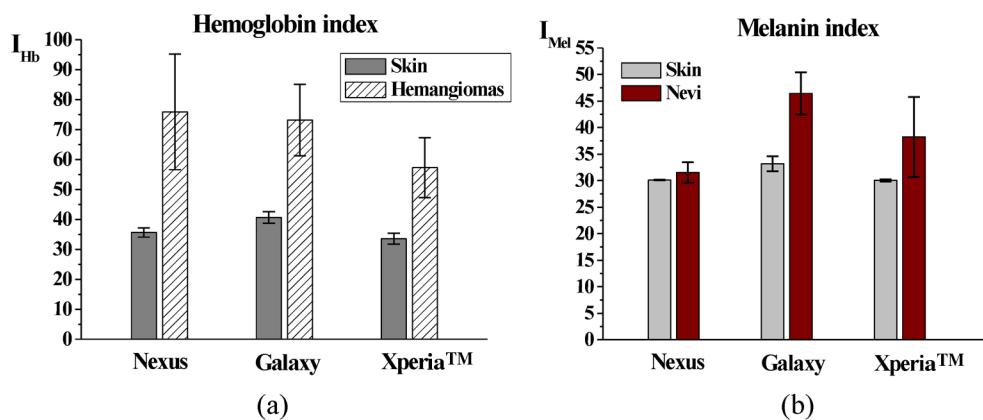


Fig. 4 (a) Hemoglobin and (b) melanin indices of skin lesions obtained by different smartphones.

#### 4 Conclusions

Three smartphones of different manufacturers were tested *in vitro* and *in vivo* using a specially designed RGB light source for skin diagnostics by smartphones. The source-detector geometry in our research provided uniform illumination, and spatial distribution of the detected signals was considered close to that exploited by other authors.<sup>15</sup> Simple algorithms were chosen to evaluate the light source performance in conjunction with the three smartphones. *In vitro* tests showed that hemoglobin and melanin indices increased with the concentration of absorbents in the phantoms for all smartphones, although curves had different slopes. The Nexus smartphone did not show any notable changes in the melanin index. This can be explained as a result of “embedded” automatic settings (ISO, white balance), which were impossible to switch off for this smartphone model. Therefore, each image captured in red, green, and blue light could have different settings and could not be used in the selected processing algorithms. *In vivo* tests indicated that hemangiomas had a higher hemoglobin index than healthy skin, and nevi had a higher melanin index compared to healthy skin, which is physiologically reasonable. For the Nexus smartphone, a negligible difference between the melanin indices of skin and nevi has been observed. This leads to the conclusion that smartphones with “embedded” automatic settings are not suited for tissue chromophore mapping, while those that allow switching off the automatic settings provide useful data. *In vivo* tests also indicated differences in results among smartphones

that could be explained by the different spectral sensitivities of their cameras, which have to be taken into consideration in further tests and the development of processing algorithms. Further clinical studies have to be performed for smartphone light source approbation, and more sophisticated algorithms must be used for skin chromophore mapping and correct diagnostics of skin lesions.

#### Acknowledgments

This work was supported by the European Regional Development Fund project “Innovative technologies for optical skin diagnostics” (#2014/0041/2DP/2.1.1.0/14/APIA/VIAA/015).

#### References

1. J. Ferlay et al., “Cancer incidence and mortality patterns in Europe: estimates for 40 countries in 2012,” *Eur. J. Cancer* **49**(6), 1374–1403 (2013).
2. R. L. Siegel, K. D. Miller, and A. Jemal, “Cancer statistics, 2015,” *CA: Cancer J. Clin.* **65**(1), 5–29 (2015).
3. J. K. Patel et al., “Newer technologies/techniques and tools in the diagnosis of melanoma,” *Eur. J. Dermatol.* **18**(6), 617–631 (2008).
4. K. Terstappen, O. Larkö, and A. M. Wennberg, “Pigmented basal cell carcinoma-comparing the diagnostic methods of SIAscopy and dermoscopy,” *Acta. Dermatol. Venereol.* **87**, 238–242 (2007).
5. G. Monheit et al., “The performance of MelaFind,” *Arch. Dermatol.* **147**(2), 188–194 (2011).
6. MedX Health, “SIMSYS™ - MOLEMATE™,” <http://www.medxhealth.com/simsys-molemate/> (2015).

7. MELA Sciences, "MelaFind®: FDA and CE Mark Approved," <http://melasciences.com/melafind> (2014).
8. N. V. K. Philips, "Philips Vital Signs Camera," <http://www.vitalsignscamera.com/> (2015).
9. E. Roth and K. Cherne "The Best Heart Disease iPhone and Android Apps of the Year," <http://www.healthline.com/health-slideshow/top-heart-disease-iphone-android-apps#5> (07 August 2015).
10. Skinvision, "About Skinvision," <https://www.skinvision.com/technology-skin-cancer-melanoma-mobile-app> (2015).
11. E. Jonathan and M. Leahy, "Cellular phone-based photoplethysmographic imaging," *J. Biophotonics* **4**(5), 293–296 (2011).
12. Beckman Laser Institute and Medical Clinic "Phantoms," <http://lammp.bli.uci.edu/education/phantoms.php> (2015).
13. C. H. Hung et al., "Broadband absorption and reduced scattering spectra of in-vivo skin can be noninvasively determined using  $\delta$ -P1 approximation based spectral analysis," *Biomed. Opt. Express* **6**(2), 443–456 (2015).
14. A. Bekina et al., "Skin chromophore mapping by means of a modified video-microscope for skin malformation diagnosis," *Proc SPIE* **8856**, 88562G (2013).
15. Y. L. Kuznetsov et al., "Optical diagnostics of vascular reactions triggered by weak allergens using laser speckle-contrast imaging technique," *Quantum Electron.* **44** (8), 713–718 (2014).